

Study of the origin of the unexpected pearlite during the cooling stage of two cast high-speed steels

Jérôme TCHOUFANG TCHUINDJANG^{1,a} and Jacqueline LECOMTE-BECKERS^{1, b}

¹Metallic Materials Science Unit – Aerospace & Mechanics Department. – University of Liege
IMGC, Bât. B52; 1, Chemin des Chevreuils – 4000 Liège, Belgium
^aj.tchuindjang@ulg.ac.be, ^bjacqueline.lecomte@ulg.ac.be

Key words: HSS, crystallization behaviour, carbides, phase transformations, pearlite.

Abstract. Two HSS grades (A and B) belonging to the complex system Fe-Cr-C-Si-X, where X is a strong carbide-forming element such as V, Mo or W, were studied. Samples in the as-received conditions came from an industrial spin casting process, with a varying cooling rate during processing. Chemical compositions of both alloys were closed to each other and were chosen to enhance their hardenability and to avoid less resistant phases such as pearlite and ferrite. Differential Thermal Analysis was performed on both alloys, in order to increase their crystallization behaviour. Light microscopy and SEM associated with EDS analyses were done to characterize the microstructure of both alloys in the as-received conditions and after DTA trials. The matrix of both HSS grades was composed of eutectic carbides, martensite and retained austenite, these phases exhibiting similar chemical compositions in both alloys. Unexpected pearlite was found in the as-cast HSS alloy B without W, this grade containing more Mo, more V and less Cr than the HSS grade A. It appeared from DTA tests that pearlite found in the alloy B arose more from the destabilisation of the Cr-rich retained austenite associated with the plate-like M_2C carbide, than from the matrix itself. In fact, pearlite zones located in the vicinity of M_2C are due to related isothermal solid phase transformations from the previous austenitic eutectic phase that is enriched with Cr and Mo.

Introduction

High Speed Steels alloy (HSS) are alloys belonging to the complex system Fe-C-Si-X, where X is a strong carbide forming element such as Cr, V, Nb, Mo, W, etc [1-8]. HSS alloys contain very hard carbides at grain boundaries with matrix composed of martensite or bainite in order to sustain wear and oxidation resistances in cold or hot conditions as in this the case for rolling mill applications [2, 9]. Carbides usually found in HSS are type MC, M_2C , M_7C_3 , M_6C or M_3C both pro-eutectic and eutectic ones, as they precipitate during the solidification process. Their nature mainly varies either with the chemical composition of the alloy or the cooling rate [3-7, 10-13]. The chemical composition and the casting route on HSS alloys influence dendritism and grain size, these features playing a great role on mechanical properties such as strength, wear, toughness and hardness [3-5]. For most of the previous works done on HSS alloys, the study of solidification paths seemed to be the main issue. Thus solid state transformations occurring below the solidification range are generally little or less discussed since HSS contain alloying elements which increase the hardenability of the matrix. Furthermore the expected matrix of HSS alloys in the as-cast conditions is often known to be of martensite or bainite type, with more or less retained austenite, the latter phase being transformed during subsequent heat treatments [4, 10, 14]. Maratray and Ussegliot-Nanot showed that an increase in the Cr/C ratio as well as in the Mo content improved significantly the hardenability of such alloys through the delay in incubation time for pearlitic transformation together with the precipitation of a Cr-rich fine secondary carbide inside the newly destabilised austenite matrix. Such a destabilisation of the prior austenite grain deeply influence the S and C-curves of TTT and CCT diagrams respectively [15].

This paper lays emphasis on the conditions that promote the occurrence of pearlite in the vicinity of eutectic carbide M_2C during the casting route while the matrix remains unconcerned as its austenitic phase keeps a great and expected hardenability. Such an insight of the so-called abnormal pearlite formation is enhanced by the metallurgical comparison between two HSS grades with similar casting conditions and different but closed chemical compositions.

Raw Materials

The studied alloys come from the shell material of bimetallic composite work rolls used in the rear finishing stands of the Hot Strip Mill. These rolls were obtained by a vertical spin casting process. Samples for subsequent microstructural analyses were cut out near the surface of the shell, from the earlier 25 mm in depth on the shell material.

The average composition of the studied materials is given in Table 1. HSS grade B is free of W, but contains more V, more Mo and less Cr than HSS grade A, the other alloying elements being similar in their amount for both grades.

Table 1: Average chemical composition of HSS materials [% weight]

HSS Grades	Alloying elements								
	C	Si	Mn	Ni	Cr	V	Mo	W	Fe
A	1.6	0.3	0.7	1.0	5.0 – 7.0	3.0 – 5.0	3.0 – 5.0	1.0 – 3.0	Bal.
B	2.0	0.6	1.2	1.5	3.0 – 5.0	4.0 – 6.0	5.0 – 7.0	-	

Experimental methods

Thermodynamical simulations were performed while using MTDData® software with SGTE data base. MTDData simulations assume infinitely slow variations of the temperature with free diffusion of the alloying elements either in the melt or in the solid state.

Differential Thermal Analysis (DTA) was used to help the casting route simulation through the enhancement of phase transformations during remelting and solidification sequence of the studied alloys. DTA tests were obtained on a Netzsch STA 449 device at a constant heating or cooling rates of 5°C/min.

Microstructure characterization was realised through both light microscopy, on an Olympus BX 60M apparatus, and Scanning Electron Microscopy (SEM) together with Energy Dispersive X-rays Spectroscopy (EDS), on a XL-30 FEG ESEM Philips.

Results

Equilibrium and non-equilibrium simulations. Major results obtained from equilibrium diagrams by thermodynamical simulations are given in Table 2. In the equilibrium conditions, the solidification sequence starts with the formation of γ -FCC prior to the formation of eutectic MC carbides for both HSS grades. Carbides other than MC eutectics are also predicted by equilibrium simulations, these carbides been eutectoid ones as they appear in the solid state, late below the solidus. Eutectoid carbides predicted by equilibrium conditions are M_7C_3 , M_6C and $M_{23}C_6$ HSS grade A, and only $M_{23}C_6$ type for HSS grade B.

Table 2: Important temperatures obtained from Equilibrium simulations on HSS grades A and B

Phase transformations	HSS grade A	HSS grade B
Liquidus (γ -FCC)	1330°C	1320°C
MC eutectic carbides	1260°C	
Solidus	1200°C	
M_7C_3 eutectoid carbides	1050°C	-
M_6C eutectoid carbides	1050°C	-
$M_{23}C_6$ eutectoid carbides	925°C	925°C
Ferritic transformation start, A_3 (α -BCC)	780°C	790°C
Ferritic transformation end, A_1 (α -BCC)	660°C	660°C

Non-equilibrium conditions obtained from DTA tests are illustrated on figure 1 and table 3 for the cooling mode, with the enhancement of the crystallisation behaviour of both HSS grades. Each peak of the DTA thermogram curve is related to a phase transformation.

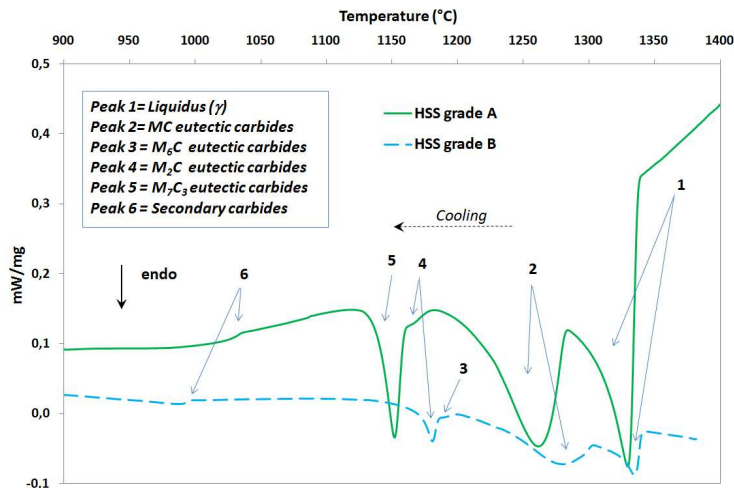


Figure 1: Crystallisation behaviour of HSS grades A and B through DTA cooling mode (DTA tests performed at 5°C/min for the cooling rate)

The same carbides like those predicted from equilibrium conditions are also present in non-equilibrium conditions, but their designations are different since all of them are eutectic ones, except for $M_{23}C_6$ which remain of eutectoid type. The temperature ranges for the solidification sequence and subsequent phase transformations in the solid state are not similar in equilibrium and non equilibrium conditions, except for the liquidus temperature on both grades.

Table 3: Important temperatures obtained from DTA experiments on HSS grades A and B

Peaks	Phase transformation designations	Peaks occurrence (T°)	
		A grade	B Grade
1 : $L \rightarrow \gamma_0$	Solidification start (Liquidus)	Yes (1340°C)	Yes (1340°C)
2 : $L \rightarrow \gamma_1 + MC$	Eutectic 1 (precipitation of V-rich carbides)	Yes (1280°C)	Yes (1305°C)
3: $L \rightarrow \gamma_4 + M_6C$	Eutectic 4 (precipitation of Mo-rich carbides)	No	Yes (1190°C)
4: $L \rightarrow \gamma_2 + M_2C$	Eutectic 2 (precipitation of Mo-rich carbides)	Yes (1175°C)	Yes (1175°C) Solidus
5: $L \rightarrow \gamma_3 + M_7C_3$	Eutectic 3 (precipitation of Cr-rich carbides)	Yes (1160°C) Solidus	No
6 : $\gamma_0 \rightarrow$ fine secondary carbides (+ γ_5)	Eutectoid 1 (precipitation of fine secondary carbides)	Yes (1030°C)	Yes (985°C)

As-cast microstructures characterisation. Micrographs obtained from the as-cast industrial conditions are given at figures 2 to 5. Optical (fig. 2 and 3) and electron (fig. 4 and 5) micrographs show a quasi continuous network of intercellular eutectic carbides at grain boundaries (GB) with a matrix composed of martensite and retained austenite (RA) for both HSS grades A and B.

3 types of eutectic carbides are present on HSS grade A in the as-cast conditions, namely petal-like V-rich MC, fishbone-like Cr-rich M_7C_3 and acicular or needle-like Mo and W-rich M_2C (fig. 2 and 4). Only MC and M_2C eutectic carbides are present on as-cast HSS grade B (fig. 3 and 5). EDS map (fig. 6b) gives an overview of the elements distribution within the studied phases on HSS grade B. Both morphology and average chemical compositions of carbides found in HSS grades A and B seem to be in good agreement with the results given in previous studies [1-9, 11-15].

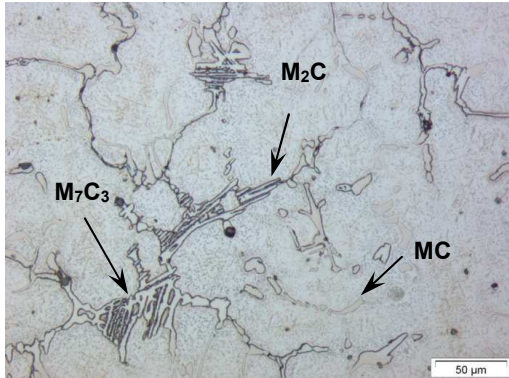


Figure 2: HSS grade A after industrial casting, showing eutectic carbides (light) at GB with a mixed martensite-RA matrix – *Nital etched*

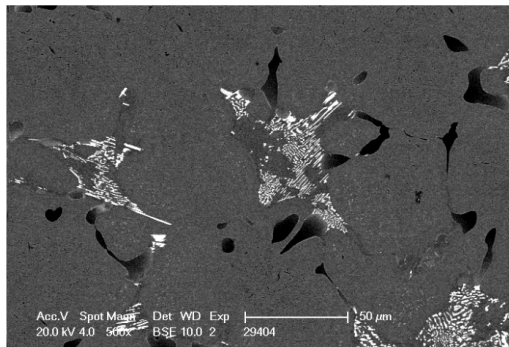


Figure 4: HSS grade A after industrial casting - Petal-like MC carbides (dark) and complex M_7C_3/M_2C carbides (light) in a martensite/RA matrix (grey) – *As polished*

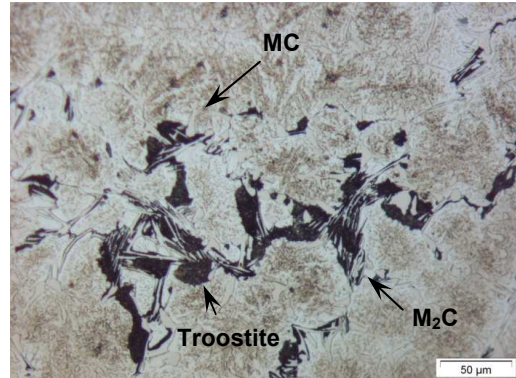


Figure 3: HSS grade B after industrial casting showing eutectic carbides at GB, troostite (dark) in the vicinity of M_2C carbides, and martensite-RA matrix – *Nital etched*

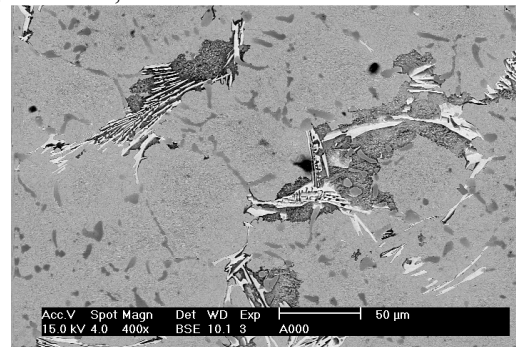


Figure 5: HSS grade B after industrial casting with Petal-like MC carbides (dark), Acicular M_2C carbides (light) with neighbouring troostite (dark grey) in a martensite/RA matrix – *Nital etched*

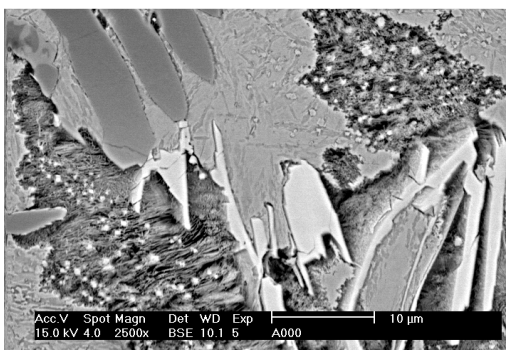


Figure 6a: Microstructure of HSS grade B in as-cast conditions, with the enhancement of the troostite fine lamellar structure located in the vicinity of M_2C carbides; very fine Mo-rich carbides are fully dispersed within the troostite – *Nital etched*

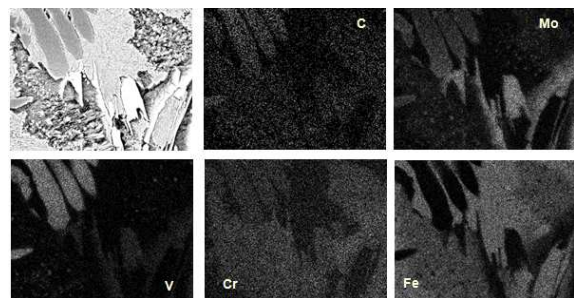


Figure 6b: EDS map related to figure 6a showing the distribution of major elements on MC carbides (V-rich), M_2C carbides (Mo-rich), and troostite (Cr-rich); there are small Mo-rich precipitates within the troostite

Compared to HSS grade A, HSS grade B in the as-cast conditions does not contain Cr-rich M_7C_3 carbides but exhibits an additional phase also known as troostite (fig. 3, 5 and 6a), a very fine pearlite. The troostite found in HSS grade B is Cr-rich and it contains very fine Mo-rich secondary carbides that are fully dispersed within this phase (fig. 6a). Furthermore, this troostite seems to be always located in the vicinity of M_2C eutectic carbides (fig. 3, 5 and 6a).

Discussion

Equilibrium versus Non-Equilibrium. It appears from DTA tests that non-equilibrium conditions lead to a microstructure different from the one predicted by equilibrium thermodynamical simulations. The following statements can be made:

- Only one eutectic carbide (MC) is predicted by equilibrium diagram instead of the three types (MC, M_2C and M_7C_3) found in HSS grade A, or the two types (MC and M_2C) found in HSS grade B;
- Neither the modification in alloying elements nor equilibrium or non-equilibrium conditions do affect the liquidus temperature, which appears similar for both HSS grades (around 1330°C). But there is a shift of the solidus point to lower temperatures when moving from equilibrium conditions to non-equilibrium ones;
- The decrease of the solidus temperature in the non-equilibrium conditions is related to the modification of the M_2C and M_7C_3 carbides types from eutectoid ones in the equilibrium simulations to eutectic ones in the non-equilibrium ones.
- The actual solidus temperature of HSS grade A appears lower than that of the HSS grade B as M_7C_3 eutectic carbides precipitated only in the former HSS grade, and these carbides precipitated after the M_2C type which is present in both HSS grades.

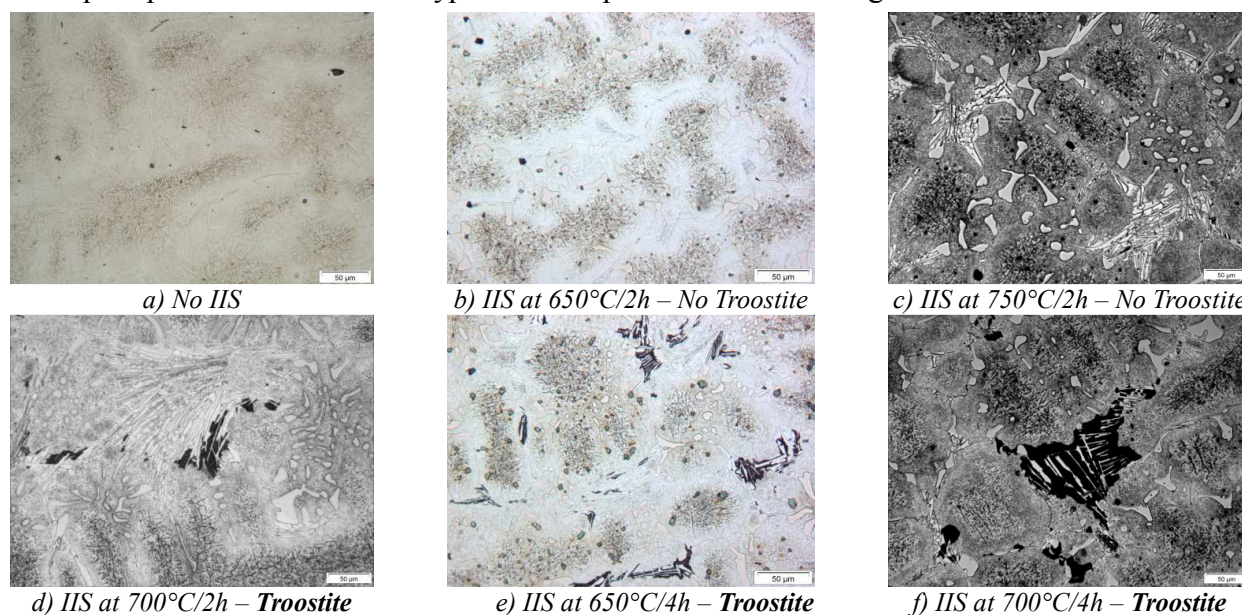


Figure 7 a) to f): Optical micrographs showing the occurrence of troostite in HSS grade B as a function of temperature and holding time when an Isothermal Intermediate Stage (IIS) is set within the continuous cooling sequence of DTA test (cooling rate of 5°C/min) – Nital etched

Mixed CCT-TTT conditions for troostite occurrence. As no troostite was found after classical DTA tests performed at a constant cooling rate of 5°C/min on HSS grade B, others trials were made on the same alloy to simulate a complete solidification sequence starting from the melt down to room temperature, either at faster (20 and 10°C/min) or lower cooling rates (2 and 1°C/min). These trials did not allow the formation of pearlite. It is the reason why the constant cooling rate of 5°C/min during DTA tests was changed to introduce an Intermediate Isothermal Stage (IIS), this level been intercalated in the overall cooling sequence. The temperature of the IIS was chosen respectively at 800, 750, 700, 650, 600 and 500°C with a holding time of 2 or 4 hours, to allow the interception of a possible pearlitic nose in the unknown isothermal diagram of such an alloy. Major results of tests with ISS are illustrated by the optical micrographs of figure 7.

For a 2 hours holding time on the ISS during the DTA cooling sequence, troostite was found only on the sample with ISS set at 700°C. For a 4 hours holding time on the ISS, the 650°C sample exhibited troostite whereas the 750°C sample did not. Meanwhile, an increase of the holding time from 2 h to 4 h led to an increase of the troostite amount in the 700°C sample.

Whenever troostite occurred, this phase was still located closed to M_2C carbides (fig 7d to 7f), like it had been previously seen in the industrial as-cast HSS grade B samples (fig 3 and 5).

Thus it could be assumed that the “pearlitic nose” for the mixed CCT-TTT conditions is closed to 700°C as the incubation time for troostite occurrence is minimal for this temperature. The real incubation time remains unknown but could be considered lower or equal to 2h.

Furthermore, it is suggested that the enrichment in Cr and Mo of the eutectic austenite associated with M_2C carbides in HSS B during the solidification stage is responsible of the formation of the latter troostite through a pseudo continuous cooling sequence with an ISS. It could also been assumed that fine Mo-rich secondary carbides found in the troostite result from the precipitation of a certain amount of Mo and C previously contained in the parent eutectic austenitic phase associated with M_2C carbide when such a phase undergoes eutectoid transformation. On the same time, the bulk austenitic grain remained untransformed till the martensitic point is reached.

Conclusions

A slight variation in major alloying elements could modify the solidification path, especially the occurrence of eutectic carbides. In fact, three types of eutectic carbides were found in HSS grade A namely V-rich MC, Mo and W-rich M_2C and Cr-rich M_7C_3 , these carbides precipitating in the corresponding sequence. HSS grade B with more Mo, more V and less Cr than HSS A, contains only MC and M_2C eutectic carbides.

Equilibrium simulations allow a partial prediction of actual solidification paths, as only the liquidus temperature and the occurrence of MC eutectics carbides were found similar either for equilibrium and non equilibrium simulations in both HSS grades, while the predicted solidus temperature was higher than the actual one obtained from non equilibrium experiments.

The austenite associated with M_2C to form the eutectic phase in HSS grade B contains more Cr and more Mo than that of HSS grade A. As a consequence, this austenite undergoes an eutectoid transformation during the industrial cooling sequence, leading to the formation of troostite in the vicinity of M_2C carbides. In the same time the bulk austenitic grain remains untransformed.

References

- [1] T. Okane and T Umeda: *Sci. and Tech. of Adv. Mater.* 2 (2001), p. 247
- [2] Y. Pan, H. Yang, X. Liu and X. Bian: *Mater. Letters* 58 (2004), p. 1912
- [3] C. K. Kim, J. Il Park, S. Lee, Y. C. Kim, N. J. Kim and J. S. Yang: *MMT A36* (2005), p. 87
- [4] J. Lecomte-Beckers, J. T. Tchuindjang, E. Pirard and J-P. Breyer: *Stal'* Vol. 2 (2003), p. 88
- [5] W. Shizhong, Z. Jinhua, X. Liuji and L. Rui: *Mat. and Design* 27 (2006), p. 58
- [6] F. Pan, M. Hirohashi, Y Lu, P. Ding, A. Tang and D. V. Edmonds: *MMT A35* (2004), p. 2757
- [7] L. A. Dobrzanski, A. Zarychta and M Ligarski: *Jrn. of Mater. Proc. Tech.* 63 (1997), p. 531
- [8] M. Boccalini and H. Goldenstein: *Internat. Mater. Rev.* Vol. 46 No.2 (2001), p. 92
- [9] M. Hashimoto, O. Kubo and Y. Matsubara: *ISIJ Intern.* Vol. 44 No. 2 (2004), p. 372
- [10] J. Lecomte-Beckers and J. T. Tchuindjang: *Def. and Diff. Forum* Vol. 289-292 (2009), p. 77
- [11] J. D. B. DeMello, M. Durand-Charre and S. Hamar-Thibault: *Met. Tr.* 14A (1983), p. 1793
- [12] H. F. Fischmeister, R. Riedl and S. Karagöz: *Met. Trans.* 20A (Oct. 1989), p. 2133
- [13] J. Lecomte-Beckers and J. T. Tchuindjang: *GIT – Imaging and Microscopy* Vol. 2 (2005), p. 2
- [14] B. Decaudin, C. Djega-Mariadassou and G. Cizeron: *Jrn. of All. and Comp.* 226 (1995), p. 208
- [15] F. Maratray and R; Usseglio-Nanot: *Facteurs affectant la structure des fontes blanches au chrome et au chrome-molybdène*, edited by Climax Molybdenum S.A., Paris, France

Solid-Solid Phase Transformations in Inorganic Materials

doi:10.4028/www.scientific.net/SSP.172-174

Study of the Origin of the Unexpected Pearlite during the Cooling Stage of Two Cast High-Speed Steels

doi:10.4028/www.scientific.net/SSP.172-174.803